STRUCTURAL CHEMISTRY
ISSN 2053-2296

# Ammonium bis(salicylaldehyde thiosemicarbazonato)ferrate(III), a supramolecular material containing low-spin $Fe^{III}$

Robyn E. Powell,[a,b] Berthold Stöger,[c] Christian Knoll,[d] Danny Müller,[d] Peter Weinberger[d] and Petra J. van Koningsbruggen[a,b]*

[a]School of Engineering and Applied Science, Chemical Engineering and Applied Chemistry, Aston University, Aston Triangle, Birmingham B4 7ET, West Midlands, UK, [b]Aston Institute of Materials Research, Aston University, Birmingham B4 7ET, West Midlands, UK, [c]X-ray Center, Vienna University of Technology, Getreidemarkt 9, 1060 Vienna, Austria, and [d]Institute of Applied Synthetic Chemistry, Vienna University of Technology, Getreidemarkt 9/163-01-3, 1060 Vienna, Austria. *Correspondence e-mail: p.vankoningsbruggen@aston.ac.uk

Received 18 March 2020
Accepted 13 May 2020

Edited by A. R. Kennedy, University of Strathclyde, Scotland

**Keywords:** ammonium; iron(III); crystal structure; low spin; order-disorder; maximum degree of disorder; MDO.

**CCDC reference**: 2003812

**Supporting information**: this article has supporting information at journals.iucr.org/c

The synthesis and crystal structure (100 K) of the title compound, ammonium bis[salicylaldehyde thiosemicarbazonato(2−)-$\kappa^3O,N^1,S$]iron(III), $NH_4[Fe(C_8H_7N_3OS)_2]$, is reported. The asymmetric unit consists of an octahedral $[Fe^{III}(thsa)_2]^-$ fragment, where $thsa^{2-}$ is salicylaldehyde thiosemicarbazonate(2−), and an $NH_4^+$ cation. Each $thsa^{2-}$ ligand binds *via* the thiolate S, the imine N and the phenolate O donor atoms, resulting in an $Fe^{III}S_2N_2O_2$ chromophore. The ligands are orientated in two perpendicular planes, with the O and S atoms in *cis* and the N atoms in *trans* positions. The $Fe^{III}$ ion is in the low-spin state at 100 K. The crystal structure belongs to a category I order–disorder (OD) family. It is a polytype of a maximum degree of order (MDO). Fragments of the second MDO polytype lead to systematic twinning by pseudomerohedry.

## 1. Introduction

The study of the coordination chemistry of thiosemicarbazones is an attractive research area. Thiosemicarbazones display a wide range of pharmacological uses based, for example, on their antineoplastic, antibacterial, antiviral and antifungal activities (Beraldo & Gambino, 2004; Yemeli Tido *et al.*, 2010). This pharmacological action is often related to coordination of the thiosemicarbazone to metal ions (Farrell, 2002). On the other hand, the magnetic properties of iron(III) compounds of thiocarbazone derivatives have attracted attention, particularly as switching behaviour was displayed for iron(III) bound to particular salicylaldehyde thiosemicarbazone derivatives (van Koningsbruggen *et al.*, 2004; Phonsri *et al.*, 2017; Powell *et al.*, 2014, 2015; Yemeli Tido, 2010; Zelentsov *et al.*, 1973, Ryabova *et al.*, 1978, 1981*a*,*b*, 1982; Floquet *et al.*, 2003, 2006, 2009; Li *et al.*, 2013).

This type of magnetic interconversion between the low-spin ($S=\frac{1}{2}$) and high-spin ($S=\frac{5}{2}$) state in $Fe^{III}$ ($3d^5$) systems has now been found to be triggered by a change in temperature or pressure, or by light irradiation (Hayami *et al.*, 2000, 2009; van Koningsbruggen *et al.*, 2004) and may be used in a functional way in research and technology (Létard *et al.*, 2004; Gütlich *et al.*, 2004; Gütlich & Goodwin 2004; van Koningsbruggen *et al.*, 2004; Nihei *et al.*, 2007; Halcrow, 2013; Harding *et al.*, 2016).

In recent years, particular interest has focused on $Fe^{III}$ complexes of substituted derivatives of *R*-salicylaldehyde 4*R*′-thiosemicarbazone (Powell *et al.*, 2014, 2015; Yemeli Tido, 2010; Floquet *et al.*, 2003, 2006, 2009; Li *et al.*, 2013) for generating $Fe^{III}$ spin crossover. In solution, free *R*-salicyl-

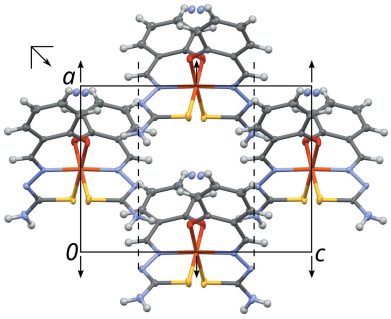

aldehyde 4$R'$-thiosemicarbazone ($H_2L$) exists in two tautomeric forms, *i.e.* the thione and thiol forms, as illustrated in Scheme 1. The chemistry of the $Fe^{III}$ compounds is rather complicated as it is possible for the tridentate *R*-salicylaldehyde 4$R'$-thiosemicarbazone ligand ($H_2L$) to exist in tautomeric forms; moreover, the ligand may also be present in its neutral, anionic or dianionic form. However, the formation of a particular type of $Fe^{III}$ complex unit, *i.e.* neutral, monocationic or monoanionic, can be achieved by tuning the degree of deprotonation of the ligand through pH variation of the reaction solution during the synthesis (Powell *et al.*, 2014, 2015; Powell, 2016; Yemeli Tido, 2010; Floquet *et al.*, 2009). We have been particularly skilled in preparing anionic $Fe^{III}$ complexes of the general formula (cation$^+$)[Fe($L^{2-}$)$_2$]·*x*(solvent), for which it became evident that the electronic state of the $Fe^{III}$ ion is dependent on the nature of the counter-ion, the nature and degree of solvation and the nature of the *R*,*R'*-substituted ligands (Powell *et al.*, 2014, 2015; Powell, 2016; Yemeli Tido, 2010).

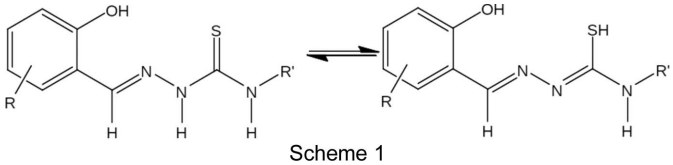


Scheme 1

We report here a novel $Fe^{III}$ compound, ammonium bis[salicylaldehyde thiosemicarbazonato(2−)-$\kappa^3O,N^1,S$]iron(III), (I) (see Scheme 2), containing two dianionic tridentate ligands, *i.e.* salicylaldehyde thiosemicarbazonate(2−), abbreviated as thsa$^{2-}$, whose structure was determined at 100 K. Ryabova *et al.* (1981*a*) reported the crystallographic data of the related compound Cs[Fe(thsa)$_2$] at 103 and 298 K, which contains $Fe^{III}$ in the high-spin electronic state ($S = \frac{5}{2}$). The main difference between $NH_4$[Fe(thsa)$_2$] and Cs[Fe(thsa)$_2$] is the associated outer-sphere cation. This article describes that the variation in the cation leads to a modification of the structure of the $Fe^{III}$ compound, also changing the crystal packing, and being responsible for the $Fe^{III}$ in the present $NH_4$[Fe(thsa)$_2$] compound exhibiting the low-spin electronic state ($S = \frac{1}{2}$).

Compound (I) systematically crystallizes as twins. The twinning will be interpreted in the light of order–disorder (OD) theory (Dornberger-Schiff & Grell-Niemann, 1961). The OD theory was created in the 1950s to explain the common occurrence of polytypism and stacking faults. It has since been developed into a comprehensive theory of local/partial symmetry. According to OD theory, if a structure is composed of layers and the layers are related by partial symmetry that is not valid for the whole structure, then the stacking becomes ambiguous. This means that the layers can be arranged in different ways, which are nevertheless all locally equivalent. Owing to the short range of interatomic interactions, these different stacking arrangements are also energetically equivalent. Consequently, OD structures often feature stacking faults. In OD twins, such as the title compound, the stacking faults lead to domains with different spacial orientations and are sporadic, *i.e.* the resulting domains are macroscopic and do not diffract coherently.

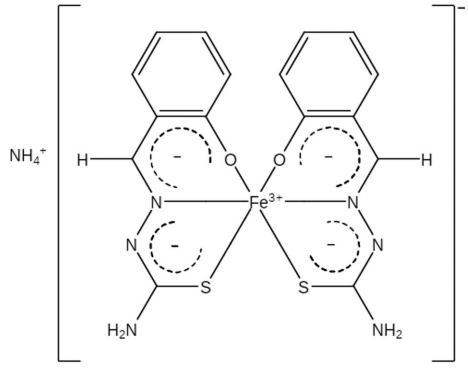


(I)

Scheme 2

## 2. Experimental

### 2.1. Spectroscopic measurements

Room-temperature IR spectra within the range 4000–400 cm$^{-1}$ were recorded on a PerkinElmer FT–IR spectrometer Spectrum RXI using KBr pellets. Variable-temperature FT–IR spectra were measured with the attenuated total reflectance (ATR) technique using a PerkinElmer spectrum 400 with a Harrick diamond ATR equipped with a thermostatable temperature-control device. $^1$H and $^{13}$C{$^1$H} NMR spectra were recorded on a Bruker 200 spectrometer with a broadband probe head. All NMR chemical shifts are reported in ppm; $^1$H and $^{13}$C shifts are established on the basis of the residual solvent resonance.

### 2.2. Synthesis and crystallization

The synthesis of $H_2$thsa was carried out according to the general procedure described by Yemeli Tido (2010). Salicylaldehyde (49 mmol, 5.98 g) was dissolved in ethanol (80 ml) with constant stirring, and was added to a solution of thiosemicarbazide (49 mmol, 3.68 g) in ethanol (40 ml). The corresponding mixture was refluxed for 120 min. The resulting solution was cooled to room temperature and the solid isolated by filtration, washed with ether and dried in a vacuum for 2 d (yield: 7.75 g, 39.7 mmol, 81.0%; m.p. 491 K). $H_2$thsa is soluble in methanol, acetone and dimethyl sulfoxide (DMSO). $^1$H NMR (200 MHz, DMSO-$d_6$): $\delta$ (ppm) 11.39 (*s*, 1H, NH), 9.84 (*s*, 1H, OH), 8.40 (*s*, 1H, CH), 8.10 (*s*, 1H, *o*-ArCH), 7.87 (*d*, $J$ = 8.8 Hz, 2H, NH$_2$), 7.19 (*t*, $J$ = 7.7 Hz, 1H, *p*-ArCH), 6.92–6.71 (*m*, 2H, *m*-ArCH). $^{13}$C NMR (50 MHz, DMSO-$d_6$): $\delta$ (ppm) 177.76 (C═S), 156.52 (C—OH), 140.16 (C═N), 131.31 (ArCH), 126.99 (ArCH), 120.33 (ArCH), 119.48 (ArCH), 116.22 (ArCH). IR (cm$^{-1}$, KBr): 3445 ($\nu$OH), 3175 ($\nu$NH), 3319 ($\nu$NH$_2$), 1616 ($\nu$C═N), 1540–1603 ($\nu$C═C), 1266 ($\nu$C—N), 1111 ($\nu$C═S).

For the synthesis of $NH_4$[Fe(thsa)$_2$], (I), Fe(*p*-$CH_3C_6H_4SO_3$)$_3$·6$H_2O$ (1.0 mmol, 0.68 g) was dissolved in methanol (5 ml). $H_2$thsa (1.0 mmol, 0.20 g) was dissolved in methanol (25 ml) with the addition of $NH_4OH$ (20 ml, 35 wt% in water). To this mixture, the methanolic solution of the $Fe^{III}$ salt was added dropwise with constant stirring. The resulting dark-

**Table 1**
Experimental details.

| | |
|---|---|
| Crystal data | |
| Chemical formula | $(NH_4)[Fe(C_8H_7N_3OS)_2]$ |
| $M_r$ | 460.34 |
| Crystal system, space group | Monoclinic, $P2_1/n$ |
| Temperature (K) | 100 |
| $a, b, c$ (Å) | 8.4393 (8), 18.2444 (17), 11.7635 (11) |
| $\beta$ (°) | 90.052 (4) |
| $V$ (Å$^3$) | 1811.2 (3) |
| $Z$ | 4 |
| Radiation type | Mo $K\alpha$ |
| $\mu$ (mm$^{-1}$) | 1.09 |
| Crystal size (mm) | 0.60 × 0.36 × 0.18 |
| Data collection | |
| Diffractometer | Bruker Kappa APEXII CCD |
| Absorption correction | Multi-scan (*SADABS*; Bruker, 2012) |
| $T_{min}$, $T_{max}$ | 0.601, 0.746 |
| No. of measured, independent and observed [$I > 2\sigma(I)$] reflections | 62618, 5355, 4839 |
| $R_{int}$ | 0.041 |
| (sin $\theta/\lambda)_{max}$ (Å$^{-1}$) | 0.708 |
| Refinement | |
| $R[F^2 > 2\sigma(F^2)]$, $wR(F^2)$, $S$ | 0.042, 0.110, 1.10 |
| No. of reflections | 5355 |
| No. of parameters | 274 |
| No. of restraints | 4 |
| H-atom treatment | H atoms treated by a mixture of independent and constrained refinement |
| $\Delta\rho_{max}$, $\Delta\rho_{min}$ (e Å$^{-3}$) | 0.93, −0.74 |

Computer programs: *APEX2* (Bruker, 2012), *SAINT-Plus* (Bruker, 2012), *SUPERFLIP* (Palatinus & Chapuis, 2007), *SHELXL2018* (Sheldrick, 2015) and *ORTEP-3* (Farrugia, 2012).

green solution was stirred and heated to 353 K for approximately 10 min. The solution was then allowed to stand at room temperature until crystals had formed. The dark-green microcrystals were isolated by filtration and dried (yield: 0.10 g, 0.22 mmol, 21.7%). Elemental analysis found/calculated (%) for $C_{16}H_{18}FeN_7O_2S_2$: C, 41.47/41.47, H 3.90/3.94, N 20.99/21.30, O 8.05/6.95, S 13.87/13.93. IR (cm$^{-1}$, KBr): 3472, 3240 ($\nu$NH), 3016 ($\nu NH_2$), 1595 ($\nu$C═N), 1546–1509 ($\nu$C═C ring), 1278 ($\nu$C—O), 1203 ($\nu$N—N), 1027 ($\nu$C—N), 756 ($\nu$C—S).

### 2.3. Refinement

Crystal data, data collection and structure refinement details are summarized in Table 1. The crystal was modelled as twinned by reflection at (100). The positions of the H atoms on the amine N atoms were located in difference Fourier maps and were refined with restrained N—H distances of 0.87 (2) Å. The $NH_4^+$ cation is disordered around a pseudo-twofold axis. The ammonium N atom was refined as disordered about two positions (N7 and N7′). The sum of the occupancy parameters was constrained to 1. The atomic displacement parameters (ADPs) were constrained to the same value, resulting in a significant decrease of the estimated standard uncertainty on the occupancy parameters. Even though residual electron density in the difference Fourier maps could be attributed to the H atoms of the disordered ammonium positions, a reliable refinement was not possible. The ammonium H atoms were therefore ultimately omitted from the refinement. Other H atoms were included in the refinement in calculated positions and allowed to ride on their parent atoms.

## 3. Results and discussion

### 3.1. Crystal structure

The structure of $NH_4[Fe(thsa)_2]$, (I) (Fig. 1), was determined at 100 K and was found to crystallize in the monoclinic space group $P2_1/n$. The asymmetric unit consists of one formula unit, *i.e.* $NH_4[Fe(thsa)_2]$, with no atom on a special position. The $Fe^{III}$ cation is coordinated by two dianionic *O*,*N*,*S*-tridentate chelating $thsa^{2-}$ ligands, displaying a distorted octahedral $Fe^{III}O_2N_2S_2$ geometry. Selected geometric parameters are listed in Table 2. The twofold deprotonated ligands are coordinated to the $Fe^{III}$ atom *via* the phenolate O, thiolate S and imine N atoms. These donor–$Fe^{III}$ bonds are located in two perpendicular planes, with the O and S atoms in *cis* positions, whereby the S1—Fe—S2 and O1—Fe—O2 angles are 92.07 (3) and 88.53 (12)°, respectively. In addition, the N atoms are situated in *trans* positions, which is evidenced by the N1—Fe—N4 bond angle of 176.71 (11)°. The $FeO_2N_2S_2$ coordination core is distorted; the Fe–donor atom distances fall within the range expected for $Fe^{III}$ in the low-spin state (van Koningsbruggen *et al.*, 2004).

The incorporation of a monovalent $NH_4^+$ cation could be corroborated by variable-temperature FT–IR spectroscopy, which revealed the sharpening of the N—H stretching vibrational mode of the $NH_4^+$ cation at 3240 cm$^{-1}$ upon cooling from ambient temperature to 173 K, which is in line with the freezing of the rotation of the $NH_4^+$ cation in the cavity.

The presence of the trivalent iron cation is supported by the coordination of two doubly deprotonated ligands to the $Fe^{III}$

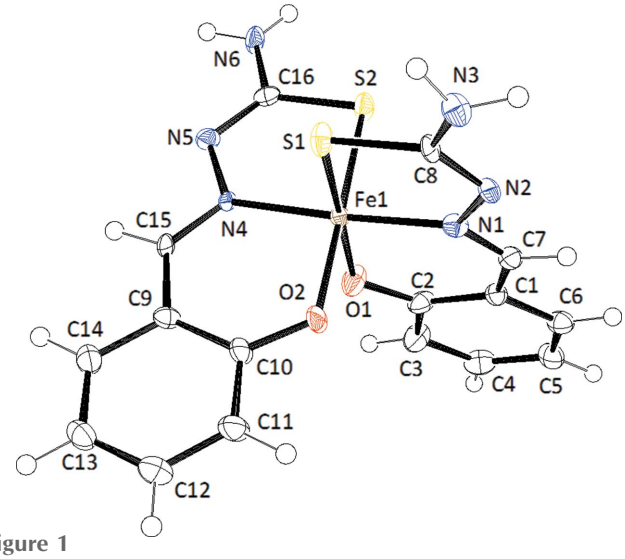


**Figure 1**
The molecular structure and atom-numbering scheme for $NH_4[Fe(thsa)_2]$, (I). The N atom of the $NH_4^+$ cation has been omitted for clarity. Displacement ellipsoids are drawn at the 50% probability level.

**Table 2**
Selected geometric parameters (Å, °).

| | | | |
|---|---|---|---|
| Fe1—N1 | 1.937 (3) | S1—C8 | 1.745 (3) |
| Fe1—O1 | 1.941 (3) | S2—C16 | 1.747 (3) |
| Fe1—N4 | 1.944 (3) | N1—C7 | 1.295 (4) |
| Fe1—O2 | 1.952 (3) | N1—N2 | 1.398 (4) |
| Fe1—S1 | 2.2369 (10) | N4—C15 | 1.293 (4) |
| Fe1—S2 | 2.2377 (10) | N4—N5 | 1.406 (4) |
| | | | |
| N1—Fe1—O1 | 93.08 (11) | C16—S2—Fe1 | 95.57 (12) |
| N1—Fe1—N4 | 176.71 (11) | C2—O1—Fe1 | 126.5 (2) |
| O1—Fe1—N4 | 88.73 (11) | C10—O2—Fe1 | 126.4 (2) |
| N1—Fe1—O2 | 88.97 (11) | C7—N1—Fe1 | 125.7 (2) |
| O1—Fe1—O2 | 88.53 (12) | C8—N2—N1 | 113.4 (3) |
| N4—Fe1—O2 | 93.83 (11) | C15—N4—Fe1 | 125.0 (2) |
| N1—Fe1—S1 | 86.44 (9) | C16—N5—N4 | 113.7 (3) |
| O1—Fe1—S1 | 177.74 (10) | C2—C1—C7 | 122.4 (3) |
| N4—Fe1—S1 | 91.85 (9) | O1—C2—C1 | 124.5 (3) |
| O2—Fe1—S1 | 89.26 (10) | N1—C7—C1 | 126.9 (3) |
| N1—Fe1—S2 | 91.60 (9) | N2—C8—S1 | 124.7 (2) |
| O1—Fe1—S2 | 90.15 (9) | C10—C9—C15 | 124.2 (3) |
| N4—Fe1—S2 | 85.65 (9) | O2—C10—C9 | 123.6 (3) |
| O2—Fe1—S2 | 178.59 (10) | N4—C15—C9 | 126.4 (3) |
| S1—Fe1—S2 | 92.07 (3) | N5—C16—S2 | 124.0 (3) |
| C8—S1—Fe1 | 94.63 (11) | | |

ion. In addition, the presence of both dianionic ligands is confirmed by the C—S, C—N and N—N bond lengths (Table 2) obtained for $NH_4[Fe(thsa)_2]$, which show characteristics of a bond order between single and double bonds. Ryabova *et al.* (1981*a*) reported the structure of the related high-spin compound $Cs[Fe(thsa)_2]$ at 103 and 298 K, which crystallizes in the space group $Pna2_1$ with an asymmetric unit consisting of a $Cs^+$ cation and an $[Fe(thsa)_2]^-$ anionic unit. The C—S, C—N and N—N bond lengths [at 103 K: C—S = 1.749 (9) and 1.761 (9) Å; C—N = 1.314 (10) and 1.303 (11) Å; N—N = 1.371 (11) and 1.380 (11) Å; at 298 K: C—S = 1.743 (14) and 1.775 (17) Å; C—N = 1.281 (19) and 1.281 (19) Å; N—N = 1.393 (18) and 1.412 (18) Å] reported by Ryabova *et al.* (1981*a*) for $Cs[Fe(thsa)_2]$, correspond to the bond lengths for $NH_4[Fe(thsa)_2]$, (I), at 100 K.

The hydrogen-bonding interactions of $NH_4[Fe(thsa)_2]$ are listed in Table 3 and are displayed in Fig. 2. The terminal N atoms of the tridentate ligands (N3 and N6), form N6—HN62···O2$^{i}$ and N3—HN32···O1$^{ii}$ contacts with the phenolate donor atoms O1 and O2, respectively. In this manner, successive $Fe^{III}$ entities are linked in the *c* direction. The $NH_4^+$ cations are distributed in between the layers of the $Fe^{III}$ entities, with alternate separations of the N atoms of the $NH_4^+$ cation of 3.915 (7) [at $(x+1, y, z)$, denoted iii] and 4.547 (7) Å [at $(x+\frac{1}{2}, -y+\frac{1}{2}, z+\frac{1}{2})$, denoted iv] in the *a* direction. The $Fe^{III}\cdots Fe^{III}$ separations in the present compound are 8.4393 (8) Å for $Fe^{III}\cdots Fe^{III_{iii}}$ and 9.7134 (13) Å for $Fe^{III}\cdots Fe^{III_{v}}$ [symmetry code: (v) $-x, -y+1, -z+1$]. The $Fe^{III}$ units in $NH_4[Fe(thsa)_2]$ are linked by hydrogen-bonding interactions between the corresponding phenolate O and amino N atoms of the $Fe^{III}$ units.

The embedding of the $NH_4^+$ cation is, therefore, essentially different from that of the $Cs^+$ cation in $Cs[Fe(thsa)_2]$ at 103 and 298 K, where the nearest-neighbour coordination sphere of the $Cs^+$ cation is constituted by O, N and C atoms, which form a seven-pointed polyhedron with Cs–(ligand donor

**Table 3**
Hydrogen-bond geometry (Å, °).

| *D*—H···*A* | *D*—H | H···*A* | *D*···*A* | *D*—H···*A* |
|---|---|---|---|---|
| N3—HN31···O1$^{i}$ | 0.87 (2) | 2.03 (3) | 2.879 (4) | 164 (6) |
| N6—HN62···O2$^{ii}$ | 0.88 (2) | 1.96 (2) | 2.834 (4) | 178 (5) |

Symmetry codes: (i) $x-\frac{1}{2}, -y+\frac{1}{2}, z+\frac{1}{2}$; (ii) $x-\frac{1}{2}, -y+\frac{1}{2}, z-\frac{1}{2}$.

atom) separations between 3.06 and 3.82 Å (Ryabova *et al.*, 1981*a*). This feature shows some similarity with the $Cs^+$ cation in $Cs[Fe(5\text{-Br-thsa})_2]$ (Powell *et al.*, 2015) that is at the centre of an irregular seven-donor-atom polyhedron, the donor atoms of which originate from symmetry-related equivalents of both symmetry-independent 5-bromosalicylaldehyde thiosemicarbazonate(2−) (5-Br-thsa) ligands. Several donor atoms coordinated to the $Fe^{III}$ atom of $Cs[Fe(5\text{-Br-thsa})_2]$ form interactions with the $Cs^+$ cation in the second coordination sphere; this is likely to modulate the electron density of the Fe–(donor atom) bonds and hence influence the electronic state of the $Fe^{III}$ cation. The latter is also prone to be affected by the assembly of $Fe^{III}$ units in the unit cell. The presence of the Br substituent on the salicylaldehyde group of the ligand in $Cs[Fe(5\text{-Br-thsa})_2]$ is a factor in determining the crystal packing, as the Br substituent of one $Cs[Fe(5\text{-Br-thsa})_2]$ unit provides a hydrogen-bonding interaction with an amino group of a neighbouring $Fe^{III}$ unit, creating ring systems.

Clearly, the variation in cation, ligand substituents and crystal packing is related to the spin state of $Fe^{III}$ being high-spin in $Cs[Fe(thsa)_2]$ at 103 and 298 K (Ryabova *et al.*, 1981*a*), low-spin in $Cs[Fe(5\text{-Br-thsa})_2]$ at 293 K (Powell *et al.*, 2015)

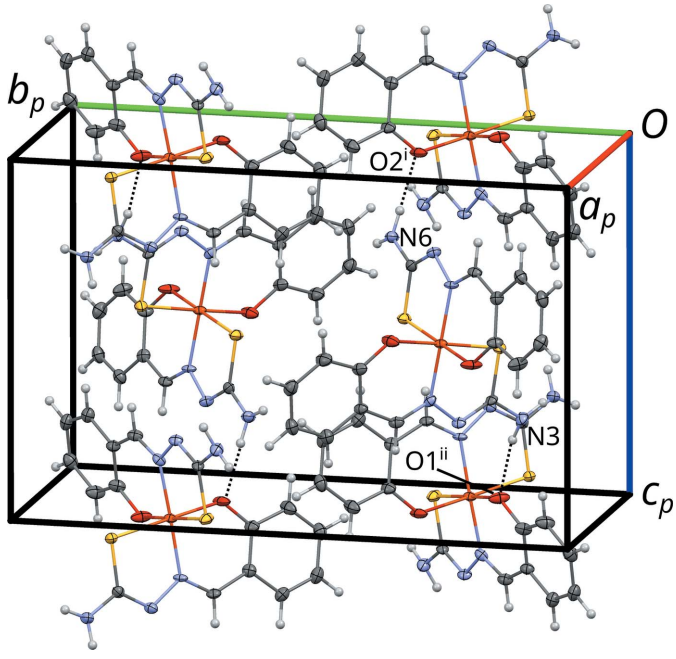


**Figure 2**
A projection showing the unit cell of $NH_4[Fe(thsa)_2]$, (I). The N atom of the $NH_4^+$ cation has been omitted for clarity. Displacement ellipsoids are drawn at the 50% probability level. Dashed lines indicate hydrogen bonds. [Symmetry codes: (i) $x-\frac{1}{2}, -y+\frac{1}{2}, z-\frac{1}{2}$; (ii) $x-\frac{1}{2}, -y+\frac{1}{2}, z+\frac{1}{2}$.]

and low-spin in the present $NH_4[Fe(thsa)_2]$ at 100 K. Variable-temperature magnetic susceptibility measurements (10–300 K) confirm that the $Fe^{III}$ ion in $NH_4[Fe(thsa)_2]$ remains in the low-spin state over this temperature range (Powell, 2016). In addition, within this family of cation(+) bis[*R*-salicylaldehyde 4*R*′-thiosemicarbazonato(2−)]ferrate(III) salts, the presence of particular solvent molecules may further affect the crystal packing, with the associated intermolecular effects influencing the electronic structure of $Fe^{III}$, *e.g.* leading to a low-spin state of $Fe^{III}$ in $Cs[Fe(L)_2]\cdot CH_3OH$ [*L* = 3-ethoxysalicylaldehyde 4-methylthiosemicarbazonate(2−)] at 100 K (Powell *et al.*, 2014). Our further studies of members of this $Fe^{III}$ family may shed more light on how the spin state of $Fe^{III}$ may be tuned in these systems.

### 3.2. Systematic twinning and OD theory

Even though $NH_4[Fe(thsa)_2]$ crystallizes in the monoclinic space group $P2_1/n$, the lattice is metrically virtually orthorhombic primitive [$oP$, $\beta$ = 90.052 (4)°]. The crystals are systematically twinned by the additional symmetry of the lattice with respect to the 2/*m* point symmetry of the crystal. Thus, the twin law comprises the operations {$2_{[100]}$, $m_{[100]}$, $2_{[001]}$, $m_{[001]}$} and the twin point group (Nespolo, 2004) is $2'/m'2/m2'/m'$. Since the reflections of both domains overlap nearly perfectly (twin index 1, twin obliquity ∼0), the twinning can be classified as being by *metric pseudomerohedry* (Nespolo & Ferraris, 2000).

A higher point symmetry of the lattice compared to the point symmetry of the crystal is often associated with twinning. However, it is not a sufficient precondition for its existence. In fact, many polar structures do not form twins by inversion despite inversion being an intrinsic symmetry of any lattice. One common and often overlooked cause of twinning is partial symmetry, which may lead to a twin interface that is locally equivalent to the twin individuals. The order–disorder (OD) theory (Dornberger-Schiff & Grell-Niemann, 1961) was introduced in the 1950s to deal precisely with these kinds of structures.

In the light of OD theory, the crystal structure of $NH_4[Fe(thsa)_2]$ can be decomposed into OD layers $A_n$ (*n* being a sequential number) parallel to (010), which, in this case, also correspond to layers in the crystallochemical sense (Fig. 3). The crucial point of an OD structure is that partial symmetry operations relate individual layers, yet need not be valid for the whole structure. In the case of $NH_4[Fe(thsa)_2]$, the $A_n$ layers possess (idealized) $P2(n)a$ symmetry (Fig. 4). In this layer-group notation, which is commonly used in the OD literature, the parentheses indicate the direction missing translational symmetry. The $[Fe(thsa)_2]^-$ ions are located on the twofold axes of the $A_n$ layers, whereas the ammonium ions are disordered about these axes.

The set of partial symmetry operations of any possible stacking of $NH_4[Fe(thsa)_2]$ is described by the OD groupoid family symbol (Dornberger-Schiff & Grell-Niemann, 1961).

$$\begin{matrix} P\ 2\ (n)\ a \\ n_{2,r}\ 2_2\ 2_{r-1} \end{matrix}$$

OD groupoid families are the analogue of space group types in classical crystallography. They abstract from metric parameters and additionally of the particular stacking. The first line of the symbol indicates the layer symmetry, the second line one set of operations relating adjacent layers. Since the intrinsic translations are not limited to those found in space groups, a generalization of the Hermann-Mauguin notation is used. For example, $n_{2,r}$ represents a glide reflection with the intrinsic translation $\mathbf{b}/2 + r\mathbf{c}/2$, whereby *r* is one of the metric parameters the OD groupoid family abstracts from.

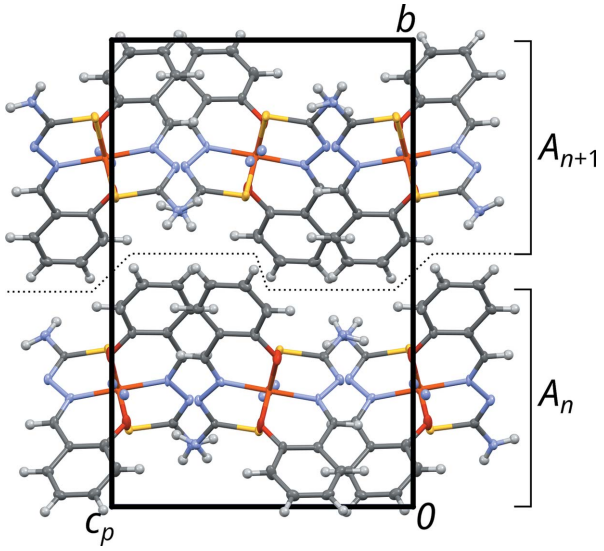


**Figure 3**
The crystal structure of $NH_4[Fe(thsa)_2]$, viewed down [100]. The names of the OD layers are indicated to the right and a dotted line indicates the interface between the OD layers, which in this case is not planar.

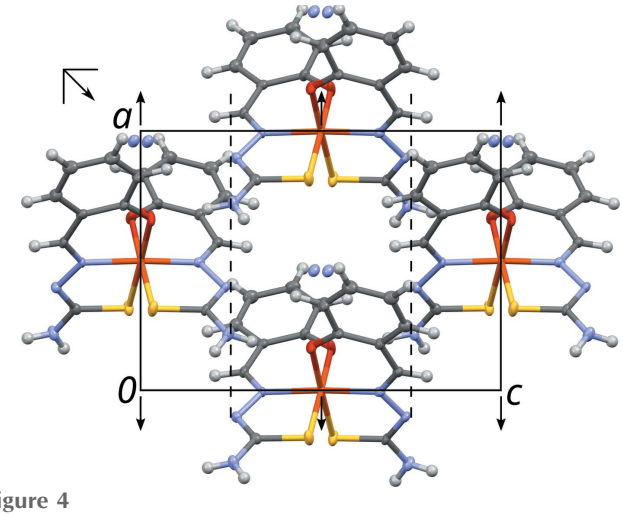


**Figure 4**
A layer in the crystal structure of $NH_4[Fe(thsa)_2]$ projected on the layer plane (010). Symmetry elements are represented by the usual graphical symbols. The indicated unit cell corresponds to the standard origin choice of the $P2(n)a$ layer group (on $2_{[100]}$), not of the overall crystal structure.

Owing to the partial symmetry, layers can be arranged in different ways while keeping pairs of adjacent layers geometrically equivalent. These stacking possibilities can be enumerated using the *NFZ* relationship (Ďurovič, 1997), which reads as $Z = N/F = [G_n{:}G_n \cap G_{n+1}]$. $G_n = P1(1)a$ is the group of operations of the $A_n$ layer that do not invert $A_n$ with respect to the stacking direction. Since the *a*-glide planes of adjacent layers do not overlap, $G_n \cap G_{n+1} = P1(1)1$. The possible layer arrangements are determined by coset decomposition of the latter in the former. In other words, given the $A_n$ layer, the adjacent $A_{n+1}$ layer can be placed in $Z = [P1(1)a{:}P1(1)1] = 2$ ways, which are related by the *a*-glide reflection of the $A_n$ layer.

Of the infinity of the thus obtained locally equivalent polytypes, a finite number is especially simple in the sense that they cannot be decomposed into fragments of even simpler polytypes. In these polytypes, which are said to be of a maximum degree of order (MDO), not only pairs but also triples, quadruples and generally *n*-tuples of adjacent layers are equivalent (for a more rigorous definition, see Dornberger-Schiff, 1982). Polytypes of the MDO type play a special role in OD theory, because all other polytypes can be decomposed into fragments of MDO polytypes. Moreover, experience shows that ordered bulk polytypes are in most cases of the MDO type. The OD family of $NH_4[Fe(thsa)_2]$ contains two MDO polytypes:

$$\mathrm{MDO_1}: P2/b11,\ \mathbf{b} = 2\mathbf{b}_0 + r\mathbf{c}$$
$$\mathrm{MDO_2}: P2_1/n,\ \mathbf{b} = 2\mathbf{b}_0$$

where $\mathbf{b}_0$ is the vector perpendicular to the layer lattices with the length of one layer width. Both MDO polytypes are shown schematically in Fig. 5. The twin individuals of $NH_4[Fe(thsa)_2]$ correspond to the $MDO_2$ polytype. A fragment of the $MDO_1$ polytype is located at the twin interface.

Thus, the OD theory plausibly explains the formation of the observed twins, as the twin interface is geometrically and, if interactions over one layer width are ignored, also energetically equivalent to the twin individuals. Moreover, it explains the pseudo-*oP* metrics of the lattice. Such a metric pseudosymmetry has often been considered as 'accidental'. However, here it is clearly very much intrinsic to the structure family.

Finally, it should be noted that an OD description is usually based on a certain degree of idealization. Ordered polytypes are desymmetrized with respect to the ideal description (Ďurovič, 1979). Indeed, in the actual $MDO_2$ polytypes of $NH_4[Fe(thsa)_2]$, the symmetry of the $A_n$ layers is reduced by an index of 2 from $P2(n)a$ to $P1(n)1$. Accordingly, the site symmetry of the $[Fe(thsa)_2]^-$ ion is reduced from 2 to 1. Moreover, the unit-cell parameters deviate slightly from orthorhombic metrics [$\beta$ = 90.052 (4)°, according to single-crystal diffraction]. Finally, the desymmetrization is also observed by a splitting of the single disordered ammonium position into two independent positions, which are now not forcibly disordered in a 1:1 manner. Indeed, the ratio of the occupancies of both positions refines to 52.7 (9):47.3 (9). However, collectively the deviations from the idealized partial symmetry are minute and the OD description can be considered as correct.

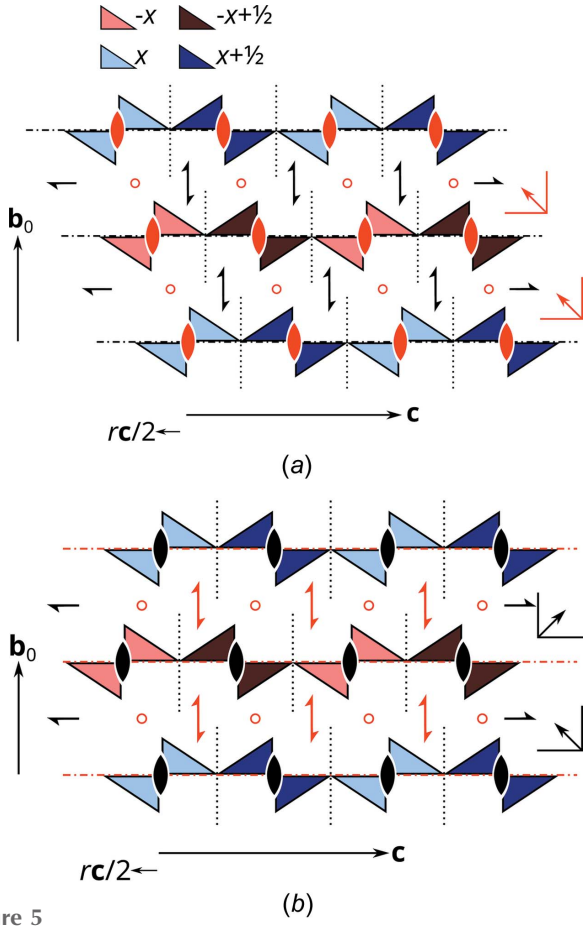


**Figure 5**
Schematic representation of the (top) $MDO_1$ and (bottom) $MDO_2$ polytypes of $NH_4[Fe(thsa)_2]$. $[Fe(thsa)_2]^-$ ions are represented by pairs of triangles which are blue on one side and red on the other side. Darker colours indicate a translation by **a**/2. The geometrical elements of partial symmetry operations of layers and those relating adjacent layers are represented by the usual graphical symbols for symmetry elements. Screw axes and glide planes with nonstandard intrinsic translations are represented using the symbols for the $2_1$ and *n* symmetry elements. Symbols of operations that are valid for the whole polytype are shown in red.

## Acknowledgements

Elemental analysis was performed at the Microanalytical Laboratory, Vienna University. PW thanks the Distinguished Visitor Fund of Aston University enabling his research visits to Aston University. The Austrian Science Fund (FWF) is kindly acknowledged for financial support for PW. PvK thanks the TU Wien International Office for financial support for her research visits to the TU Wien.

## Funding information

Funding for this research was provided by: Austrian Science Fund (project No. P 31076).

## References

Beraldo, H. & Gambino, D. (2004). *Med. Chem.* **4**, 31–39.

Bruker (2012). *APEX2* and *SAINT-Plus*. Bruker AXS Inc., Madison, Wisconsin, USA.
Dornberger-Schiff, K. (1982). *Acta Cryst.* A**38**, 483–491.
Dornberger-Schiff, K. & Grell-Niemann, H. (1961). *Acta Cryst.* **14**, 167–177.
Ďurovič, S. (1979). *Krist. Tech.* **14**, 1047–1053.
Ďurovič, S. (1997). *EMU Notes in Mineralogy*, Vol. 1, edited by S. Merlino, pp. 3–28. Jena, Germany: European Mineralogical Union.
Farrell, N. (2002). *Coord. Chem. Rev.* **232**, 1–4.
Farrugia, L. J. (2012). *J. Appl. Cryst.* **45**, 849–854.
Floquet, S., Boillot, M. L., Rivière, E., Varret, F., Boukheddaden, K., Morineau, D. & Négrier, P. (2003). *New J. Chem.* **27**, 341–348.
Floquet, S., Guillou, N., Négrier, P., Rivière, E. & Boillot, M. L. (2006). *New J. Chem.* **30**, 1621–1627.
Floquet, S., Muñoz, M. C., Guillot, R., Rivière, E., Blain, G., Réal, J. A. & Boillot, M. L. (2009). *Inorg. Chim. Acta*, **362**, 56–64.
Gütlich, P. & Goodwin, H. A. (2004). *Top. Curr. Chem.* **233**, 1–47.
Gütlich, P., van Koningsbruggen, P. J. & Renz, F. (2004). *Struct. Bond.* **107**, 27–75.
Halcrow, M. A. (2013). In *Spin-Crossover Materials: Properties and Applications*, 1st ed. Chichester: John Wiley & Sons Ltd.
Harding, D. J., Harding, P. & Phonsri, W. (2016). *Coord. Chem. Rev.* **313**, 38–61.
Hayami, S., Gu, Z., Shiro, M., Einaga, Y., Fujishima, A. & Sato, O. (2000). *J. Am. Chem. Soc.* **122**, 7126–7127.
Hayami, S., Hiki, K., Kawahara, T., Maeda, Y., Urakami, D., Inoue, K., Ohama, M., Kawata, S. & Sato, O. (2009). *Chem. Eur. J.* **15**, 3497–3508.
Koningsbruggen, P. J. van, Maeda, Y. & Oshio, H. (2004). *Top. Curr. Chem.* **233**, 259–324.
Létard, J. F., Guionneau, P. & Goux-Capes, L. (2004). *Top. Curr. Chem.* **235**, 221–249.
Li, Z. Y., Dai, J. W., Shiota, Y., Yoshizawa, K., Kanegawa, S. & Sato, O. (2013). *Chem. Eur. J.* **19**, 12948–12952.
Nespolo, M. (2004). *Z. Kristallogr.* **219**, 57–71.
Nespolo, M. & Ferraris, G. (2000). *Z. Kristallogr.* **215**, 77–81.
Nihei, M., Shiga, T., Maeda, Y. & Oshio, H. (2007). *Coord. Chem. Rev.* **251**, 2606–2621.
Palatinus, L. & Chapuis, G. (2007). *J. Appl. Cryst.* **40**, 786–790.
Phonsri, W., Darveniza, L. C., Batten, S. R. & Murray, K. S. (2017). *Inorganics*, **5**, 51.
Powell, R. E. (2016). PhD thesis, Aston University, Birmingham, UK.
Powell, R. E., Schwalbe, C. H., Tizzard, G. J. & van Koningsbruggen, P. J. (2014). *Acta Cryst.* C**70**, 595–598.
Powell, R. E., Schwalbe, C. H., Tizzard, G. J. & van Koningsbruggen, P. J. (2015). *Acta Cryst.* C**71**, 169–174.
Ryabova, N. A., Ponomarev, V. I., Atovmyan, L. O., Zelentsov, V. V. & Shipilov, V. I. (1978). *Koord. Khim.* **4**, 119–126.
Ryabova, N. A., Ponomarev, V. I., Zelentsov, V. V. & Atovmyan, L. O. (1981*a*). *Kristallografiya*, **26**, 101–108.
Ryabova, N. A., Ponomarev, V. I., Zelentsov, V. V. & Atovmyan, L. O. (1982). *Kristallografiya*, **27**, 81–91.
Ryabova, N. A., Ponomarev, V. I., Zelentsov, V. V., Shipilov, V. I. & Atovmyan, L. O. (1981*b*). *J. Struct. Chem.* **22**, 234–238.
Sheldrick, G. M. (2015). *Acta Cryst.* C**71**, 3–8.
Yemeli Tido, E. W. (2010). PhD thesis, University of Groningen, The Netherlands.
Yemeli Tido, E. W. Y., Faulmann, R., Roswanda, A., Meetsma, A. & van Koningsbruggen, P. J. (2010). *Dalton Trans.* **39**, 1643–1651.
Zelentsov, V. V., Bogdanova, L. G., Ablov, A. V., Gerbeleu, N. V. & Dyatlova, C. V. (1973). *Russ. J. Inorg. Chem.* **18**, 2654–2657.

# supporting information

*Acta Cryst.* (2020). C**76**, 625-631 [https://doi.org/10.1107/S2053229620006452]

## Ammonium bis(salicylaldehyde thiosemicarbazonato)ferrate(III), a supramolecular material containing low-spin $Fe^{III}$

**Robyn E. Powell, Berthold Stöger, Christian Knoll, Danny Müller, Peter Weinberger and Petra J. van Koningsbruggen**

### Computing details

Data collection: *APEX2* (Bruker, 2012); cell refinement: *APEX2* (Bruker, 2012); data reduction: *SAINT-Plus* (Bruker, 2012); program(s) used to solve structure: *SUPERFLIP* (Palatinus & Chapuis, 2007); program(s) used to refine structure: *SHELXL2018* (Sheldrick, 2015); molecular graphics: *ORTEP-3* (Farrugia, 2010); software used to prepare material for publication: *SHELXL2018* (Sheldrick, 2015).

**(I)**

*Crystal data*

$C_{16}H_{18}FeN_7O_2S_2$
$M_r$ = 460.34
Monoclinic, $P2_1/n$
$a$ = 8.4393 (8) Å
$b$ = 18.2444 (17) Å
$c$ = 11.7635 (11) Å
$\beta$ = 90.052 (4)°
$V$ = 1811.2 (3) Å$^3$
$Z$ = 4
$F(000)$ = 948
$D_x$ = 1.688 Mg m$^{-3}$
Mo $K\alpha$ radiation, $\lambda$ = 0.71073 Å
Cell parameters from 9753 reflections
$\theta$ = 2.8–30.2°
$\mu$ = 1.09 mm$^{-1}$
$T$ = 100 K
Rhombic prism, green
0.60 × 0.36 × 0.18 mm

*Data collection*

Bruker Kappa APEXII CCD diffractometer
Graphite monochromator
$\omega$– and $\varphi$–scans
Absorption correction: multi-scan (*SADABS*; Bruker, 2012)
$T_{min}$ = 0.601, $T_{max}$ = 0.746
62618 measured reflections
5355 independent reflections
4839 reflections with $I > 2\sigma(I)$
$R_{int}$ = 0.041
$\theta_{max}$ = 30.2°, $\theta_{min}$ = 1.1°
$h$ = −11→11
$k$ = −25→25
$l$ = −16→16

*Refinement*

Refinement on $F^2$
Least-squares matrix: full
$R[F^2 > 2\sigma(F^2)]$ = 0.042
$wR(F^2)$ = 0.110
$S$ = 1.10
5355 reflections
274 parameters
4 restraints
Hydrogen site location: mixed
H atoms treated by a mixture of independent and constrained refinement
$w = 1/[\sigma^2(F_o^2) + (0.0283P)^2 + 5.6668P]$ where $P = (F_o^2 + 2F_c^2)/3$
$(\Delta/\sigma)_{max} < 0.001$
$\Delta\rho_{max}$ = 0.93 e Å$^{-3}$
$\Delta\rho_{min}$ = −0.74 e Å$^{-3}$

*Special details*

**Geometry**. All esds (except the esd in the dihedral angle between two l.s. planes) are estimated using the full covariance matrix. The cell esds are taken into account individually in the estimation of esds in distances, angles and torsion angles; correlations between esds in cell parameters are only used when they are defined by crystal symmetry. An approximate (isotropic) treatment of cell esds is used for estimating esds involving l.s. planes.

**Refinement**. Refined as a 2-component twin.

Crystal data collection for $NH_4[Fe(thsa)_2]$ was carried out after attaching a single crystal to a Kapton micro mount by using perfluorinated oil and mounted on a Bruker KAPPA APEX II diffractometer equipped with a CCD detector. Data were collected at 100 K in a dry stream of nitrogen with MoK$\alpha$ radiation ($\lambda$ = 0.71073 Å). Data were reduced to intensity values using *SAINT-Plus* (Bruker, 2012) and absorption correction was applied using the multi-scan method implemented by *SADABS* (Bruker, 2012). The structure was solved using charge-flipping implemented by *SUPERFLIP* (Palatinus & Chapuis, 2007) and refined against $F^2$ with SHELX (Sheldrick, 2014).

*Fractional atomic coordinates and isotropic or equivalent isotropic displacement parameters (Å²)*

| | *x* | *y* | *z* | $U_{iso}$*/$U_{eq}$ | Occ. (<1) |
|---|---|---|---|---|---|
| Fe1 | −0.18454 (6) | 0.24824 (3) | 0.47816 (5) | 0.01283 (9) | |
| S1 | −0.36955 (12) | 0.16316 (4) | 0.51161 (7) | 0.02015 (17) | |
| S2 | −0.36760 (11) | 0.33417 (4) | 0.44372 (7) | 0.01932 (17) | |
| O1 | −0.0177 (3) | 0.31944 (16) | 0.4514 (2) | 0.0256 (6) | |
| O2 | −0.0210 (3) | 0.17473 (16) | 0.5062 (2) | 0.0269 (6) | |
| N1 | −0.1906 (3) | 0.26809 (14) | 0.6398 (2) | 0.0151 (5) | |
| N2 | −0.2879 (3) | 0.22705 (15) | 0.7119 (2) | 0.0155 (5) | |
| N3 | −0.4684 (4) | 0.13350 (17) | 0.7206 (3) | 0.0202 (6) | |
| N4 | −0.1913 (3) | 0.22967 (15) | 0.3155 (2) | 0.0135 (5) | |
| N5 | −0.2879 (3) | 0.27192 (16) | 0.2434 (2) | 0.0164 (5) | |
| N6 | −0.4642 (4) | 0.36688 (17) | 0.2347 (3) | 0.0201 (6) | |
| N7 | 0.2779 (9) | 0.2599 (4) | 0.4588 (7) | 0.0181 (8) | 0.473 (9) |
| N7′ | 0.2763 (8) | 0.2370 (4) | 0.4976 (6) | 0.0181 (8) | 0.527 (9) |
| C1 | −0.0056 (4) | 0.37125 (18) | 0.6414 (3) | 0.0168 (6) | |
| C2 | 0.0357 (4) | 0.3690 (2) | 0.5250 (3) | 0.0197 (6) | |
| C3 | 0.1472 (4) | 0.4205 (2) | 0.4859 (3) | 0.0260 (8) | |
| H3 | 0.178472 | 0.419564 | 0.408318 | 0.031* | |
| C4 | 0.2126 (4) | 0.47272 (19) | 0.5580 (3) | 0.0255 (8) | |
| H4 | 0.286056 | 0.507260 | 0.528461 | 0.031* | |
| C5 | 0.1725 (5) | 0.47535 (18) | 0.6724 (3) | 0.0227 (7) | |
| H5A | 0.217916 | 0.510869 | 0.721708 | 0.027* | |
| C6 | 0.0642 (4) | 0.42452 (19) | 0.7123 (3) | 0.0202 (7) | |
| H6 | 0.035885 | 0.425576 | 0.790412 | 0.024* | |
| C7 | −0.1138 (4) | 0.31973 (19) | 0.6915 (3) | 0.0178 (6) | |
| H7 | −0.130724 | 0.324031 | 0.771063 | 0.021* | |
| C8 | −0.3732 (4) | 0.17776 (17) | 0.6582 (3) | 0.0142 (6) | |
| C9 | −0.0054 (4) | 0.12707 (18) | 0.3156 (3) | 0.0168 (6) | |
| C10 | 0.0329 (4) | 0.12625 (19) | 0.4325 (3) | 0.0190 (6) | |
| C11 | 0.1425 (4) | 0.0731 (2) | 0.4712 (3) | 0.0255 (7) | |
| H11 | 0.168253 | 0.071316 | 0.549825 | 0.031* | |
| C12 | 0.2123 (4) | 0.02419 (19) | 0.3988 (3) | 0.0244 (8) | |
| H12 | 0.285668 | −0.010784 | 0.427276 | 0.029* | |
| C13 | 0.1755 (5) | 0.02567 (18) | 0.2828 (3) | 0.0234 (7) | |

| | | | | |
|---|---|---|---|---|
| H13 | 0.224536 | −0.008008 | 0.232264 | 0.028* |
| C14 | 0.0679 (4) | 0.07619 (19) | 0.2421 (3) | 0.0210 (7) |
| H14 | 0.042748 | 0.076766 | 0.163369 | 0.025* |
| C15 | −0.1132 (4) | 0.17866 (18) | 0.2639 (3) | 0.0164 (6) |
| H15 | −0.128169 | 0.174734 | 0.184033 | 0.020* |
| C16 | −0.3709 (4) | 0.32150 (17) | 0.2965 (3) | 0.0162 (6) |
| HN31 | −0.496 (8) | 0.154 (3) | 0.785 (3) | 0.06 (2)* |
| HN32 | −0.534 (5) | 0.104 (2) | 0.684 (4) | 0.040 (15)* |
| HN61 | −0.523 (5) | 0.400 (2) | 0.264 (4) | 0.028 (12)* |
| HN62 | −0.484 (6) | 0.355 (2) | 0.164 (2) | 0.027 (12)* |

*Atomic displacement parameters (Å²)*

| | $U^{11}$ | $U^{22}$ | $U^{33}$ | $U^{12}$ | $U^{13}$ | $U^{23}$ |
|---|---|---|---|---|---|---|
| Fe1 | 0.01120 (16) | 0.01814 (17) | 0.00915 (15) | 0.00055 (17) | 0.00122 (18) | 0.00086 (13) |
| S1 | 0.0290 (4) | 0.0192 (3) | 0.0123 (4) | −0.0058 (3) | 0.0039 (3) | −0.0012 (3) |
| S2 | 0.0272 (4) | 0.0188 (3) | 0.0120 (4) | 0.0058 (3) | −0.0018 (3) | −0.0016 (3) |
| O1 | 0.0215 (13) | 0.0417 (15) | 0.0136 (12) | −0.0145 (11) | 0.0028 (10) | −0.0018 (10) |
| O2 | 0.0283 (14) | 0.0434 (15) | 0.0091 (11) | 0.0183 (12) | −0.0018 (10) | −0.0033 (10) |
| N1 | 0.0121 (12) | 0.0176 (11) | 0.0156 (13) | −0.0010 (10) | 0.0009 (10) | 0.0042 (9) |
| N2 | 0.0137 (14) | 0.0211 (12) | 0.0117 (11) | −0.0005 (10) | 0.0040 (9) | 0.0005 (9) |
| N3 | 0.0254 (16) | 0.0178 (13) | 0.0175 (14) | −0.0029 (11) | 0.0060 (12) | 0.0008 (11) |
| N4 | 0.0120 (11) | 0.0231 (12) | 0.0055 (11) | −0.0001 (10) | 0.0000 (9) | 0.0003 (9) |
| N5 | 0.0149 (14) | 0.0206 (12) | 0.0137 (12) | 0.0020 (10) | −0.0006 (10) | 0.0021 (10) |
| N6 | 0.0257 (16) | 0.0197 (14) | 0.0148 (14) | 0.0038 (11) | −0.0040 (12) | −0.0010 (11) |
| N7 | 0.0184 (15) | 0.020 (2) | 0.016 (2) | −0.003 (2) | 0.003 (2) | −0.0010 (14) |
| N7′ | 0.0184 (15) | 0.020 (2) | 0.016 (2) | −0.003 (2) | 0.003 (2) | −0.0010 (14) |
| C1 | 0.0156 (15) | 0.0206 (14) | 0.0142 (15) | −0.0007 (12) | 0.0013 (12) | 0.0008 (11) |
| C2 | 0.0149 (14) | 0.0279 (16) | 0.0162 (15) | −0.0055 (12) | −0.0008 (12) | 0.0034 (13) |
| C3 | 0.0241 (18) | 0.0355 (19) | 0.0186 (16) | −0.0105 (14) | 0.0018 (13) | 0.0035 (14) |
| C4 | 0.0233 (19) | 0.0233 (15) | 0.0299 (19) | −0.0041 (13) | −0.0013 (14) | 0.0059 (14) |
| C5 | 0.0225 (17) | 0.0168 (14) | 0.0289 (19) | −0.0001 (13) | 0.0001 (15) | −0.0041 (12) |
| C6 | 0.0182 (15) | 0.0187 (15) | 0.0236 (17) | −0.0001 (12) | 0.0004 (13) | −0.0015 (13) |
| C7 | 0.0133 (14) | 0.0260 (15) | 0.0141 (14) | 0.0000 (12) | 0.0015 (12) | 0.0013 (12) |
| C8 | 0.0167 (13) | 0.0155 (13) | 0.0104 (14) | 0.0006 (11) | 0.0046 (12) | 0.0016 (10) |
| C9 | 0.0122 (14) | 0.0203 (14) | 0.0180 (15) | −0.0011 (11) | 0.0027 (11) | 0.0006 (12) |
| C10 | 0.0176 (15) | 0.0261 (16) | 0.0132 (15) | 0.0037 (12) | 0.0033 (12) | −0.0004 (12) |
| C11 | 0.0219 (17) | 0.0359 (19) | 0.0188 (17) | 0.0124 (14) | 0.0024 (13) | 0.0041 (14) |
| C12 | 0.0210 (19) | 0.0223 (15) | 0.030 (2) | 0.0049 (13) | 0.0035 (14) | 0.0038 (13) |
| C13 | 0.0222 (17) | 0.0184 (14) | 0.0296 (19) | 0.0007 (14) | 0.0026 (16) | −0.0051 (12) |
| C14 | 0.0213 (16) | 0.0204 (16) | 0.0214 (17) | −0.0011 (13) | 0.0019 (13) | −0.0048 (13) |
| C15 | 0.0162 (14) | 0.0225 (15) | 0.0106 (13) | −0.0007 (12) | 0.0027 (12) | −0.0011 (11) |
| C16 | 0.0159 (13) | 0.0158 (13) | 0.0168 (16) | −0.0024 (11) | −0.0022 (13) | 0.0010 (11) |

*Geometric parameters (Å, º)*

| | | | |
|---|---|---|---|
| Fe1—N1 | 1.937 (3) | N5—C16 | 1.304 (4) |
| Fe1—O1 | 1.941 (3) | N6—C16 | 1.354 (4) |

| | | | |
|---|---|---|---|
| Fe1—N4 | 1.944 (3) | C1—C6 | 1.410 (5) |
| Fe1—O2 | 1.952 (3) | C1—C2 | 1.413 (5) |
| Fe1—S1 | 2.2369 (10) | C1—C7 | 1.438 (5) |
| Fe1—S2 | 2.2377 (10) | C2—C3 | 1.408 (5) |
| S1—C8 | 1.745 (3) | C3—C4 | 1.389 (5) |
| S2—C16 | 1.747 (3) | C4—C5 | 1.389 (5) |
| O1—C2 | 1.330 (4) | C5—C6 | 1.384 (5) |
| O2—C10 | 1.320 (4) | C9—C14 | 1.412 (5) |
| N1—C7 | 1.295 (4) | C9—C10 | 1.413 (5) |
| N1—N2 | 1.398 (4) | C9—C15 | 1.443 (5) |
| N2—C8 | 1.313 (4) | C10—C11 | 1.415 (5) |
| N3—C8 | 1.355 (4) | C11—C12 | 1.367 (5) |
| N4—C15 | 1.293 (4) | C12—C13 | 1.400 (5) |
| N4—N5 | 1.406 (4) | C13—C14 | 1.380 (5) |

| | | | |
|---|---|---|---|
| N1—Fe1—O1 | 93.08 (11) | C6—C1—C7 | 118.2 (3) |
| N1—Fe1—N4 | 176.71 (11) | C2—C1—C7 | 122.4 (3) |
| O1—Fe1—N4 | 88.73 (11) | O1—C2—C3 | 117.9 (3) |
| N1—Fe1—O2 | 88.97 (11) | O1—C2—C1 | 124.5 (3) |
| O1—Fe1—O2 | 88.53 (12) | C3—C2—C1 | 117.6 (3) |
| N4—Fe1—O2 | 93.83 (11) | C4—C3—C2 | 121.6 (3) |
| N1—Fe1—S1 | 86.44 (9) | C3—C4—C5 | 121.2 (3) |
| O1—Fe1—S1 | 177.74 (10) | C6—C5—C4 | 117.8 (3) |
| N4—Fe1—S1 | 91.85 (9) | C5—C6—C1 | 122.5 (3) |
| O2—Fe1—S1 | 89.26 (10) | N1—C7—C1 | 126.9 (3) |
| N1—Fe1—S2 | 91.60 (9) | N2—C8—N3 | 118.2 (3) |
| O1—Fe1—S2 | 90.15 (9) | N2—C8—S1 | 124.7 (2) |
| N4—Fe1—S2 | 85.65 (9) | N3—C8—S1 | 117.0 (2) |
| O2—Fe1—S2 | 178.59 (10) | C14—C9—C10 | 119.3 (3) |
| S1—Fe1—S2 | 92.07 (3) | C14—C9—C15 | 116.5 (3) |
| C8—S1—Fe1 | 94.63 (11) | C10—C9—C15 | 124.2 (3) |
| C16—S2—Fe1 | 95.57 (12) | O2—C10—C9 | 123.6 (3) |
| C2—O1—Fe1 | 126.5 (2) | O2—C10—C11 | 118.3 (3) |
| C10—O2—Fe1 | 126.4 (2) | C9—C10—C11 | 118.0 (3) |
| C7—N1—N2 | 113.5 (3) | C12—C11—C10 | 121.9 (3) |
| C7—N1—Fe1 | 125.7 (2) | C11—C12—C13 | 120.0 (3) |
| N2—N1—Fe1 | 120.8 (2) | C14—C13—C12 | 119.8 (3) |
| C8—N2—N1 | 113.4 (3) | C13—C14—C9 | 121.0 (3) |
| C15—N4—N5 | 114.0 (3) | N4—C15—C9 | 126.4 (3) |
| C15—N4—Fe1 | 125.0 (2) | N5—C16—N6 | 118.6 (3) |
| N5—N4—Fe1 | 121.0 (2) | N5—C16—S2 | 124.0 (3) |
| C16—N5—N4 | 113.7 (3) | N6—C16—S2 | 117.4 (3) |
| C6—C1—C2 | 119.4 (3) | | |

*Hydrogen-bond geometry (Å, º)*

| *D*—H···*A* | *D*—H | H···*A* | *D*···*A* | *D*—H···*A* |
|---|---|---|---|---|
| C11—H11···N6$^{i}$ | 0.95 | 2.69 | 3.409 (5) | 133 |

| | | | | |
|---|---|---|---|---|
| N3—H*N*31···O1$^{ii}$ | 0.87 (2) | 2.03 (3) | 2.879 (4) | 164 (6) |
| N6—H*N*62···O2$^{iii}$ | 0.88 (2) | 1.96 (2) | 2.834 (4) | 178 (5) |

Symmetry codes: (i) $x+1/2, -y+1/2, z+1/2$; (ii) $x-1/2, -y+1/2, z+1/2$; (iii) $x-1/2, -y+1/2, z-1/2$.